

## Late Paleozoic orogeny in Alaska's Farewell terrane

Dwight C. Bradley<sup>a,\*</sup>, Julie Dumoulin<sup>a</sup>, Paul Layer<sup>b</sup>, David Sunderlin<sup>c</sup>, Sarah Roeske<sup>d</sup>, Bill McClelland<sup>e</sup>, Anita G. Harris<sup>f</sup>, Grant Abbott<sup>g</sup>, Tom Bundtzen<sup>h</sup>, Timothy Kusky<sup>i</sup>

<sup>a</sup>U.S. Geological Survey, 4200 University Dr., Anchorage, AK 99508, USA

<sup>b</sup>Department of Geology and Geophysics, University of Alaska, Fairbanks, AK 99775, USA

<sup>c</sup>Department of Geophysical Sciences, University of Chicago, Chicago, IL 60637, USA

<sup>d</sup>Department of Geology, University of California, Davis, CA 95616, USA

<sup>e</sup>Department of Geology, University of Idaho, Moscow, ID 83844, USA

<sup>f</sup>U.S. Geological Survey, Reston, VA 22092, USA

<sup>g</sup>Yukon Geological Survey, Department of Energy, Mines and Resources, Government of Yukon, Whitehorse, Yukon, Canada Y1A 2B5

<sup>h</sup>Pacific Rim Geological Consulting, Inc., P.O. Box 81906, Fairbanks, AK 99708, USA

<sup>i</sup>Department of Earth and Planetary Sciences, St. Louis University, St. Louis, MO 63103, USA

Received 5 June 2003

### Abstract

Evidence is presented for a previously unrecognized late Paleozoic orogeny in two parts of Alaska's Farewell terrane, an event that has not entered into published scenarios for the assembly of Alaska. The Farewell terrane was long regarded as a piece of the early Paleozoic passive margin of western Canada, but is now thought, instead, to have lain between the Siberian and Laurentian (North American) cratons during the early Paleozoic. Evidence for a late Paleozoic orogeny comes from two belts located 100–200 km apart. In the northern belt, metamorphic rocks dated at 284–285 Ma (three <sup>40</sup>Ar/<sup>39</sup>Ar white-mica plateau ages) provide the main evidence for orogeny. The metamorphic rocks are interpreted as part of the hinterland of a late Paleozoic mountain belt, which we name the Browns Fork orogen. In the southern belt, thick accumulations of Pennsylvanian–Permian conglomerate and sandstone provide the main evidence for orogeny. These strata are interpreted as the eroded and deformed remnants of a late Paleozoic foreland basin, which we name the Dall Basin. We suggest that the Browns Fork orogen and Dall Basin comprise a matched pair formed during collision between the Farewell terrane and rocks to the west. The colliding object is largely buried beneath Late Cretaceous flysch to the west of the Farewell terrane, but may have included parts of the so-called Innoko terrane. The late Paleozoic convergent plate boundary represented by the Browns Fork orogen likely connected with other zones of plate convergence now located in Russia, elsewhere in Alaska, and in western Canada.

Published by Elsevier B.V.

**Keywords:** Cordilleran tectonics; Alaska; Permian; Orogeny; Foreland basin; Plate reconstructions

### 1. Introduction

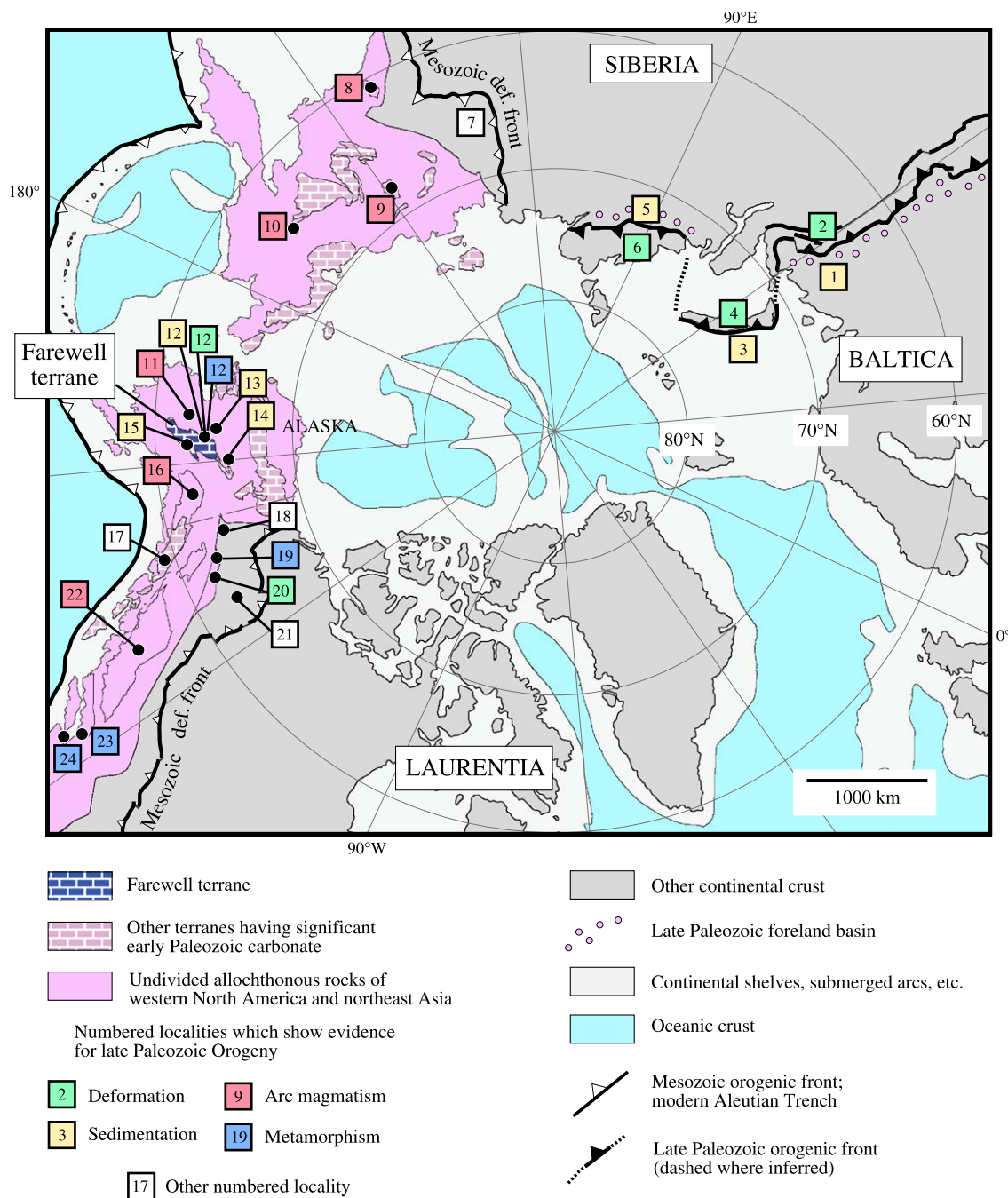
Alaska's Farewell terrane was long regarded as piece of the Paleozoic passive margin of western Canada, dislodged from its original position but not exotic to North America (e.g., locality 18 in Fig. 1)

\* Corresponding author. Tel.: +1-907-786-7434; fax: +1-907-786-7401.

E-mail address: [dbradley@usgs.gov](mailto:dbradley@usgs.gov) (D.C. Bradley).

(Coney et al., 1980; Box, 1985; Plafker and Berg, 1994). A growing body of fossil evidence now suggests, however, that the Farewell terrane lay between the Siberian and Laurentian (North American) cratons

during the early Paleozoic (Blodgett et al., 2002; Dumoulin et al., 2002). Thus, we have to question one of the foundations of most previous schemes for the assembly of Alaska, in which the Farewell terrane



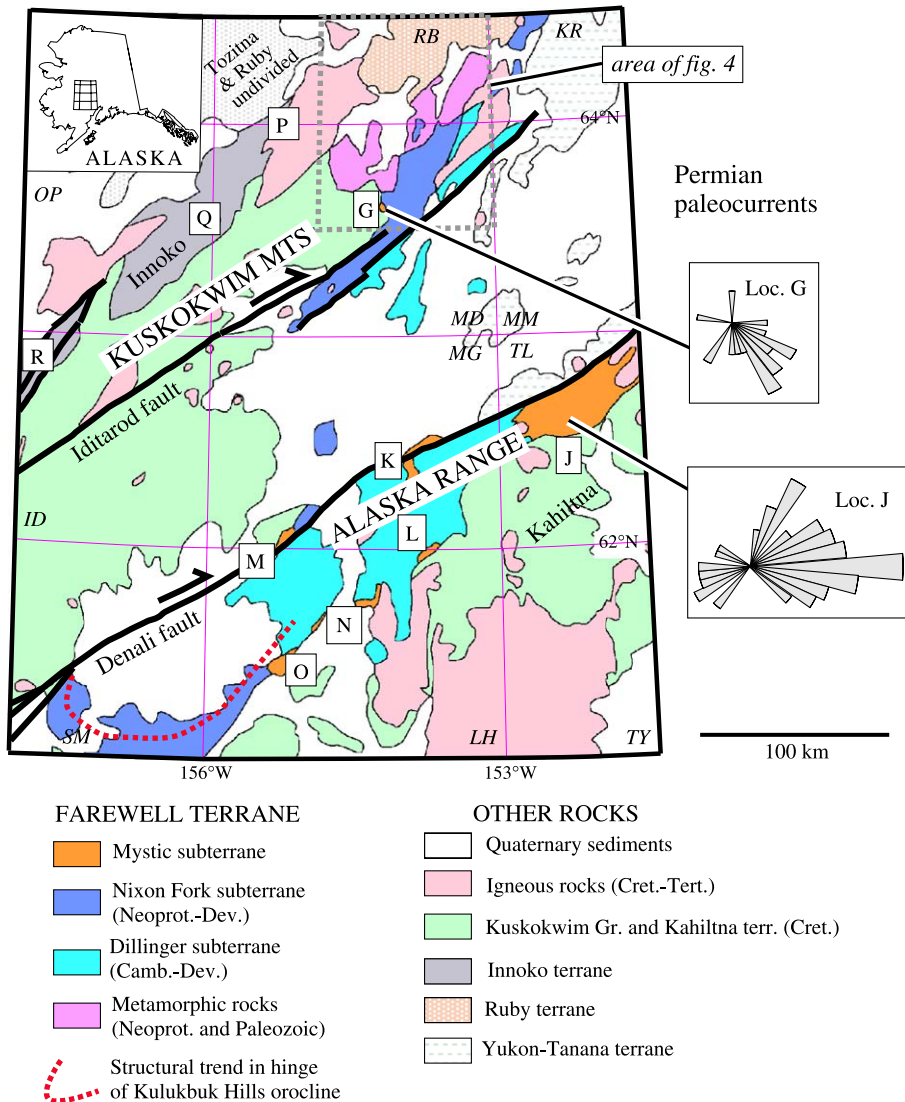


Fig. 2. Geologic map of Farewell terrane and surrounding areas, Alaska. Letters in white boxes represent localities mentioned in text. Area-proportional paleocurrent roses are based on imbricate clasts at localities G and J. Abbreviations for 1:250,000-scale quadrangle maps are: ID, Iditarod; KR, Kantishna River; LH, Lime Hills; MD, Medfra; MM, Mount McKinley; OP, Ophir; RB, Ruby; SM, Sleetmute; TL, Talkeetna; and TY, Tyonek.

Fig. 1. Map of the Arctic identifying evidence of late Paleozoic plate convergence in northwestern North America and northeastern Asia. Adapted from Sheet 19 of the Atlas Géologique du Monde (Johnson and Churkin, 1976), with modifications from Nokleberg et al. (2001). Numbered locations: 1, Uralian foredeep; 2, Northern Urals; 3 and 4, Uralian foredeep and orogen in Novaya Zemlya; 5, South Taimyr Trough (foredeep); 6, Taimyr orogen; 7, Verkhoyansk fold-thrust belt; 8, Okhotsk massif; 9, Alazeya terrane; 10, Oloy terrane; 11, Pennsylvanian volcanics in Innoko "terrane"; 12, Browns Fork orogen; 13, Permian siliciclastics in Innoko "terrane", Ruby Quadrangle; 14, Permian siliciclastics in Livengood quadrangle; 15, Dall Basin; 16, Pennsylvanian–Permian Skolai Arc, northern Wrangellia; 17, Alexander terrane; 18, original position of Farewell Terrane according to Plafker and Berg (1994); 19, Yukon–Tanana "terrane" in Ross Lake area; 20, Yukon–Tanana "terrane" in Finlayson Lake area; 21, Selwyn Basin; 22, Stikinia terrane at Stikine River, British Columbia; 23, Vedder Complex; 24, Garrison Schist.

was part of the nucleus for continental growth along North America's Cordilleran margin. The new question, then, is how and when did the Farewell terrane come to rest in Alaska's collage? The answer will require an understanding of the interactions between the Farewell terrane and each of its present neighbors (Fig. 2): the Ruby, Innoko, Yukon-Tanana, and Kahiltna, terranes, as well as other tracts buried by younger sediments.

We hereby present evidence that the assembly of this part of Alaska began with a previously unknown orogeny that affected the Farewell terrane during the Pennsylvanian and Permian. Evidence for late Paleozoic orogeny comes from two belts of rocks located 100–200 km apart. In the northern belt, metamorphic rocks provide the main evidence for orogeny; we interpret them as a vestige of the hinterland of the late Paleozoic orogen. In the southern belt, sedimentary rocks provide the main evidence for orogeny; we interpret these rocks as the eroded and deformed remnants of a late Paleozoic foreland basin.

The Farewell terrane (Fig. 2) is remote, even by Alaskan standards. It occupies an area about the size of Switzerland but is utterly inaccessible by road; the only practical access for most fieldwork is by helicopter. Parts of the Farewell terrane have been geologically mapped at scales of 1:63,360 or 1:250,000, although large areas—including the eastern half of the Ruby quadrangle, where our reconnaissance work disclosed the first evidence for the new orogeny—have never been systematically mapped, even at 1:250,000 scale.

## 2. Farewell terrane and its biogeography

The Farewell terrane<sup>1</sup> (Decker et al., 1994; Bundtzen et al., 1997a) is a continental fragment of Proterozoic to Jurassic rocks. It encompasses what various other workers have called the Nixon Fork, Dillinger, Minchumina, and Mystic terranes (Jones et al., 1987; Silberling et al., 1994; Patton et al., 1994). Decker et

al. (1994) showed how these assemblages are stratigraphically related (Fig. 3). These relationships have given rise to the subterrane nomenclature shown in Fig. 3, which is modified slightly from Bundtzen et al. (1997a). (1) A metamorphic complex, described in the next section, includes the oldest rocks of the terrane, which are Proterozoic. (2) Latest Neoproterozoic(?) through Middle Devonian platformal carbonate rocks represent the best-known part of the Farewell terrane, a passive-margin succession called the Nixon Fork subterrane. (3) A Cambrian to Lower Devonian deep-water succession of shale, chert, graywacke, and limestone is called the Dillinger subterrane. Rocks shown as Dillinger in Fig. 2 in western Mt. McKinley and eastern Medfra quadrangles were previously assigned to the Minchumina terrane (Jones et al., 1987; Silberling et al., 1994; Patton et al., 1994). Because the platformal (Nixon Fork) and deepwater (Dillinger) successions interfinger, they are not, as once believed, separate terranes (cf. Decker et al., 1994 vs. Jones et al., 1987). Until at least Devonian time, the platform lay generally west (present direction) of the deep-water basin. (4) Both the Dillinger and Nixon Fork are depositionally overlain by the Mystic subterrane (Bundtzen et al., 1997a). It includes Devonian shallow-water limestone and lesser shale and sandstone, Carboniferous to Permian sandstone, conglomerate, and minor limestone, and Triassic to Jurassic basalt and related siliciclastic rocks (Bundtzen et al., 1997a).

Shallow-water carbonate rocks of the Nixon Fork and Mystic subterrane contain fossil assemblages of mixed Siberian and Laurentian aspect (see summaries by Dumoulin et al., 2002; Blodgett et al., 2002). Cambrian trilobites, Ordovician conodonts, and Devonian brachiopods are among the fossil groups of Siberian aspect. Distinctive aphrosalpingid sponges from the Silurian of the Nixon Fork subterrane have been reported elsewhere only in the Alexander terrane of southeastern Alaska and in the Urals (Soja and Antoshkina, 1997) (Fig. 1). While differences in paleolatitude might explain some of the differences between Laurentian and Siberian shallow-water faunas, the two continents were at the same paleolatitude during a time of marked faunal difference, the Ordovician (Torsvik et al., 1995), suggesting that they were then far apart. Early Permian plant fossils from the Mystic subterrane (Mt. Dall conglomerate, dis-

<sup>1</sup> We use the term terrane in the informal, pre-1980 sense. A terrane is a tract of related rocks, with no other connotations. Where the word is set in quotes, we use "terrane" in order to conform to common usage, even though it likely includes two or more unrelated tracts of rocks.

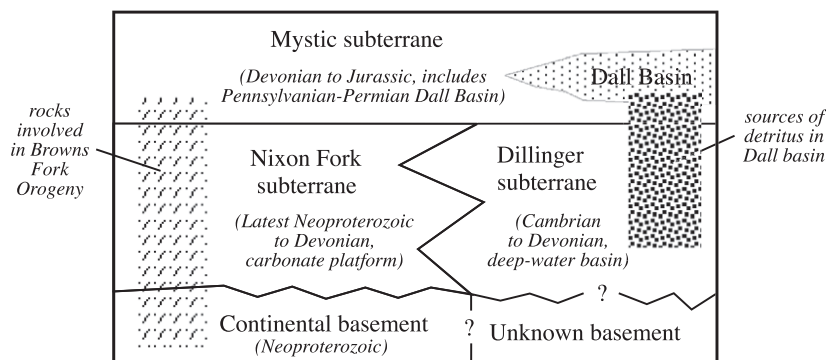


Fig. 3. Subterranean of the Farewell terrane, showing schematic relationships among the various rock sequences, and the context of late Paleozoic events discussed in this paper.

cussed below) were assigned to the Angaran (“Siberian”) realm by Mamay and Reed (1984). The biogeographic significance of the Permian floras is unclear, however, because there is no basis for comparison with northern Laurentia. In summary, the fossil record suggests that the Farewell terrane lay between the Laurentian and Siberian cratons (but separated from both) from Cambrian to at least the Devonian and possibly until after the Early Permian. One line of evidence *does* support a link between the Farewell terrane and western Canada: the lower Paleozoic stratigraphic successions of the Dillinger subterranean and Selwyn Basin (i.e., the off-shelf part of the Canadian miogeocline in the Yukon; locality 21 in Fig. 1) are similar (Bundtzen and Gilbert, 1983). If the two deep-water areas did face the same ocean, the differences between shallow-water faunas require a wide ocean.

### 3. Late Paleozoic orogeny in the northern part of the Farewell terrane (Kuskokwim Mountains)

Metasedimentary and metaigneous rocks that crop out immediately northwest of the Nixon Fork platform carbonates have been regarded as the basement of the Farewell terrane (Patton and Dutro, 1979) (Fig. 4). We present evidence for late Paleozoic metamorphism and accompanying deformation in this region. The late Paleozoic event affected both Neoproterozoic (and possibly older) rocks and the carbonates of the Nixon Fork subterranean. The U/Pb ages cited below are TIMS ages on zircon reported by McClelland et al. (1999).

The new ages reported here are from single-crystal laser step heating. The  $^{40}\text{Ar}/^{39}\text{Ar}$  methodology and data are presented in Appendices A and B. Published K/Ar and U/Pb data from this region (Silberman et al., 1979; Dillon et al., 1985) were based on methods that are now outdated.

The Precambrian rocks include three assemblages, from oldest to youngest: (1) metapelite and metabasite; (2) metarhyolite (979 and 921 Ma), quartz-mica schist, and quartzite; and (3) orthogneiss (850 Ma) (McClelland et al., 1999). *Assemblage 1.* The metapelite and metabasite (locality A in Fig. 4), which have kyanite-garnet-biotite-muscovite-quartz assemblages and hornblende-andesine assemblages, respectively, are interpreted to be the oldest rocks in this belt (pre-979 Ma). *Assemblage 2.* Metarhyolite, quartzite, and quartz-muscovite schist occur within 10 km of the kyanite schists but have not been metamorphosed beyond low greenschist grade. U/Pb zircon dates of 979 and 921 Ma on metarhyolite have been obtained from two places (localities C and D in Fig. 4). If the rhyolites are as old as 979 Ma, the kyanite-grade metamorphic event was older still. *Assemblage 3.* A nearby orthogneiss, the Baker pluton, yielded a concordant U/Pb age of 850 Ma (McClelland et al., 1999). Its contact aureole overprints the kyanite-bearing rocks. White mica from the aureole yielded  $^{40}\text{Ar}/^{39}\text{Ar}$  ages of 820 and 832 Ma (P. Layer, unpublished data). The lithology, protolith ages, and metamorphic ages of Neoproterozoic rocks of the Farewell terrane are unlike anything known from the western Canadian margin, casting yet more doubt on an original connection.

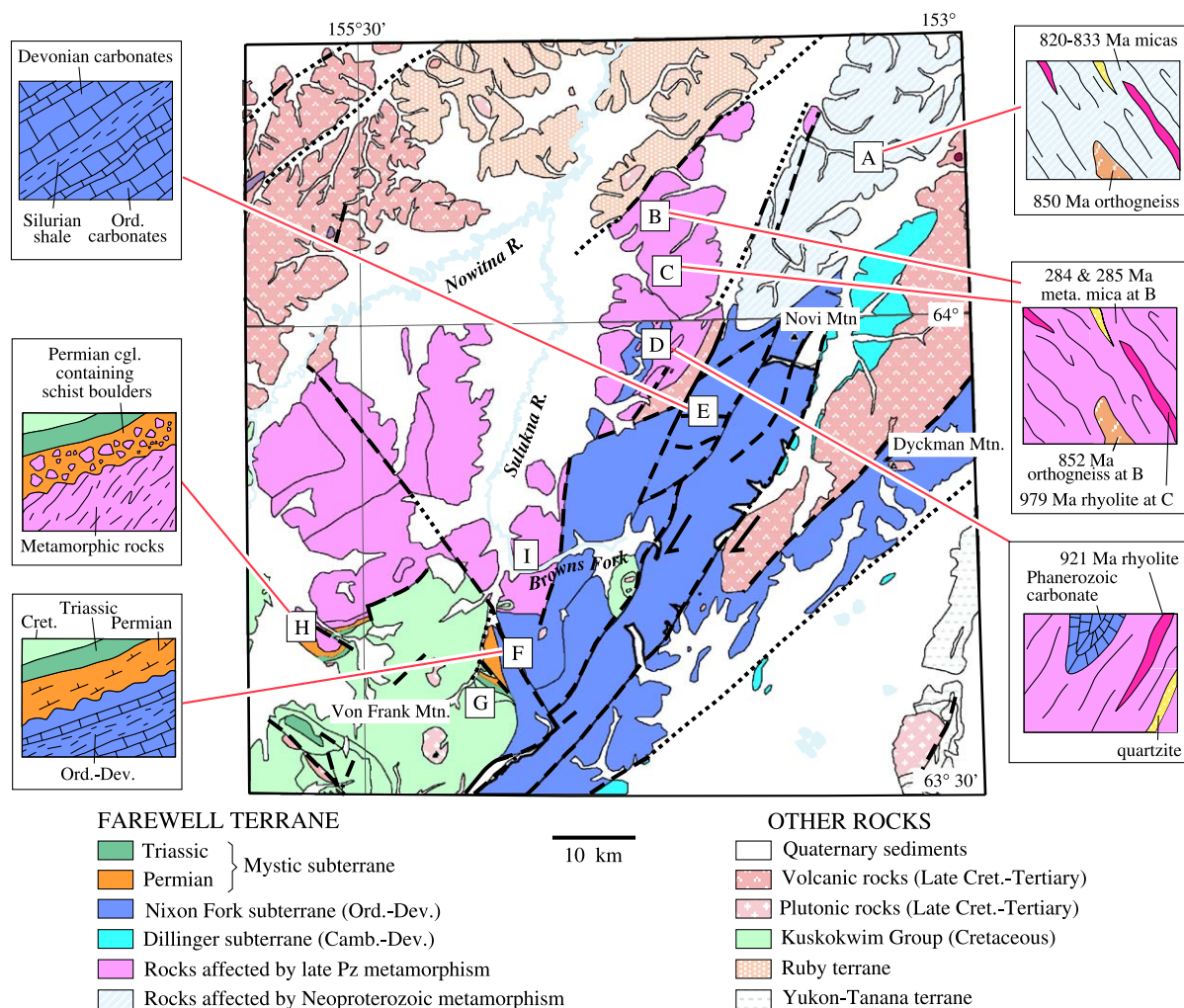


Fig. 4. Geologic map of northeastern Medfra and southeastern Ruby quadrangles, Alaska, adapted from the compilation by Wilson et al. (1998). Letters in white boxes represent localities mentioned in text. Nixon Fork carbonate rocks in the vicinity of locality D were involved in the same late Paleozoic metamorphic event as the surrounding rocks shown in purple. Insets show schematic cross-sectional relations based on reconnaissance observations.

The younger (late Paleozoic) metamorphic event is recognized on the basis of field relations, paleontology,  $^{40}\text{Ar}/^{39}\text{Ar}$  geochronology, and metamorphic textures. Our new data confirm, as Patton et al. (1980) suspected, that some of the deformed and metamorphosed rocks immediately northwest of the main part of the Nixon Fork platform are Paleozoic. At locality D (Fig. 4), marble from one exposure yielded gastropod steinkerns, indicating a Phanerozoic age; marble from a second exposure yielded a single conodont of

Middle Ordovician to Middle Devonian age. This marble unit is interlayered with pencil-cleaved phyllite containing the assemblage quartz-chlorite-muscovite-chloritoid. Three white mica separate from pelitic schist (localities B and I in Fig. 4) yielded Early Permian  $^{40}\text{Ar}/^{39}\text{Ar}$  plateau ages of 284, 285, and 285 Ma (Table 1; Fig. 6; Appendices A and B). Neoproterozoic protoliths, among them an 852-Ma orthogneiss (locality B in Fig. 4), were also involved in the late Paleozoic metamorphism. The metarhyolites

Table 1  
 $^{40}\text{Ar}/^{39}\text{Ar}$  ages of metamorphic rocks in the Ruby and Medfra quadrangles, Alaska

Sample no. and mineral	Lat/long	Integrated age (Ma)	Plateau age (Ma) <sup>a</sup>	Plateau information
2-3-1C white mica	154°07'15" 63°44'00"	282.5 ± 5.5	<b>285.4 ± 5.0</b>	6 fractions 89% $^{39}\text{Ar}$ release MSWD = 0.5
3-3-1C white mica	153°49'29" 64°08'57"	286.1 ± 5.1	<b>284.2 ± 3.4</b>	4 fractions 69% $^{39}\text{Ar}$ release MSWD = 1.5
3-7-1C white mica	153°48'42" 64°07'06"	279.6 ± 2.4	<b>285.2 ± 2.8</b>	5 fractions 88% $^{39}\text{Ar}$ release MSWD = 2.4

Analytical methods and data are given in Appendices A and B.

<sup>a</sup> Error in plateau ages includes scatter about the plateau (MSWD error).

(Fig. 5B) show a single metamorphic fabric that we interpret as late Paleozoic in age.

The area affected by Pennsylvanian–Permian metamorphism can only roughly be delineated. To the north, a boundary with Late Jurassic to Early Cretaceous blueschist-facies metamorphic rocks of the Ruby terrane (Roeske et al., 1995) probably passes somewhere through the unmapped northern part of Fig. 4. To the east, we interpret the boundary as a metamorphic front (rather than as a terrane boundary, for example) for the following reasons: outcrops that have yielded Pennsylvanian–Permian metamorphic ages (locality B in Fig. 4) lie to the west of outcrops yielding Neoproterozoic metamorphic ages (locality A in Fig. 4). Coeval zircon dates from orthogneisses in the two metamorphic tracts point to a common igneous protolith. Thus, the simplest interpretation is that the Pennsylvanian–Permian metamorphic belt was superimposed on the Neoproterozoic metamorphic belt. Accordingly, the fossiliferous marble described in the previous paragraph can be seen as a metamorphosed part of the Nixon Fork platform. Still farther east, the classic Nixon Fork carbonate succession has been folded into a series of tight to open folds, and conodonts show color alteration indices (CAI) ranging from 2 to 4.5. Some folding here was Late Cretaceous or younger (because the overlying Upper Cretaceous Kuskokwim Group is itself folded), but some folding

of the Nixon Fork strata could be as old as late Paleozoic.

The late Paleozoic metamorphic belt is flanked to the southwest by outcrops of little-deformed conglomerate which is assigned, for lack of more formal stratigraphic nomenclature, to the Mystic subterrane. The conglomerate contains large angular blocks of schist (locality H in Fig. 4) (Patton and Dutro, 1979) and its calcareous sandstone matrix has yielded a brachiopod fauna of Permian age (Patton et al., 1980). About 20 km to the east (locality F in Fig. 4), finer-grained, laterally equivalent Permian strata have been reported to depositionally overlie the Nixon Fork platform (Patton and Dutro, 1979), thus linking the Nixon Fork and the metamorphic complex by Permian time.

These field relations together support the notion that (1) the Nixon Fork platform was deposited on Neoproterozoic metamorphic basement; (2) some of the basement and some of its platformal cover were deformed and metamorphosed during the late Paleozoic; and (3) the intensity of late Paleozoic tectonism diminished eastward. A more complex alternative is that the Neoproterozoic metamorphic rocks and Nixon Fork subterrane were originally unrelated, and came together in the late Paleozoic. Either scenario involves the Farewell terrane in a late Paleozoic orogeny (Fig. 6).

#### 4. Southern part of the Farewell terrane (Alaska Range)

In the Alaska Range, 100–200 km to the south, the main evidence of late Paleozoic tectonism is sedimentary, from strata of the Mystic subterrane. A siliciclastic basin can be traced at least 200 km along regional strike and about 50 km across strike (Fig. 2, localities J, K, L, M, and N). These strata have been studied in detail at only one location, Mt. Dall (Fig. 2, locality J), where a >1500-m succession of fluvial boulder conglomerate and subordinate plant-bearing siltstone and sandstone is exposed (Fig. 5C). The conglomerate gradationally overlies a thick, Pennsylvanian(?) turbidite succession (Reed and Nelson, 1980). The conglomerate occupies a broad, open syncline, whereas the underlying, less competent flysch below is isoclinally folded. The Mt. Dall

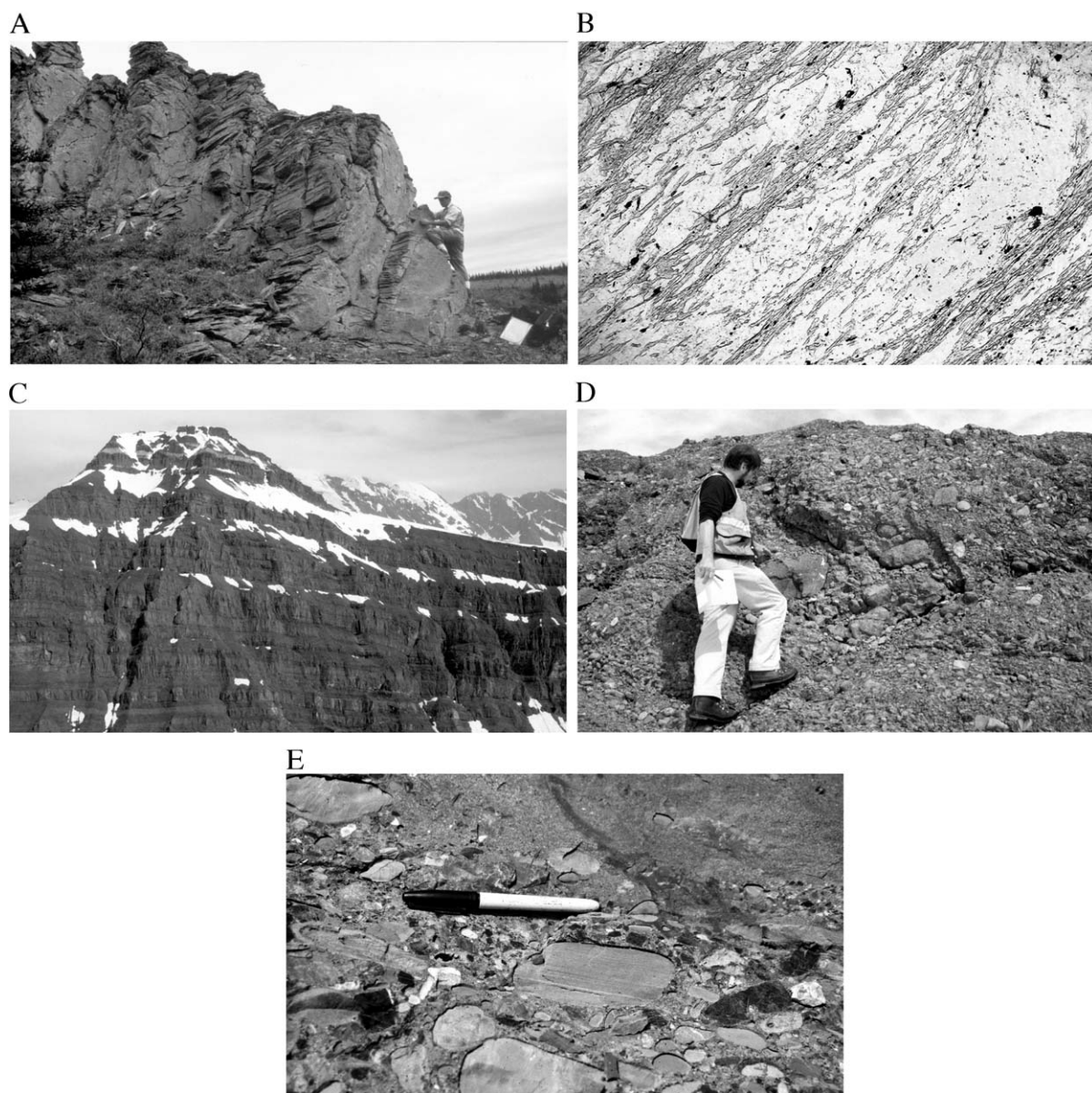


Fig. 5. (A) Outcrop of Phanerozoic marble within the late Paleozoic metamorphic belt, locality D in Fig. 4. (B) Photomicrograph of metarhyolite, locality B in Fig. 4. White mica defining the foliation yielded an age of 285 Ma. (C) View of Mt. Dall, Alaska Range, showing upper part of ~1500-m section of Lower Permian fluvial conglomerate and sandstone. (D) Outcrop of Mt. Dall conglomerate. The two largest clasts, in the middle of the photo, are of resedimented conglomerate. (E) Close-up of Mt. Dall conglomerate showing light-colored clasts of limestone from Mystic subterranean and smaller, dark clasts of chert from Dillinger subterranean.

conglomerate was assigned an Early Permian age based on its flora of ferns, pteridosperms, and the cordaite-like genus, *Zamiopteris* (Mamay and Reed, 1984). Clasts, the largest approaching 1 m in diameter,

are almost exclusively sedimentary rocks, derived from the Mystic and Dillinger subterraneans (Fig. 5D). Boulders and cobbles include radiolarian chert (53% of 501 clasts), limestone (40%), intraformational sand-

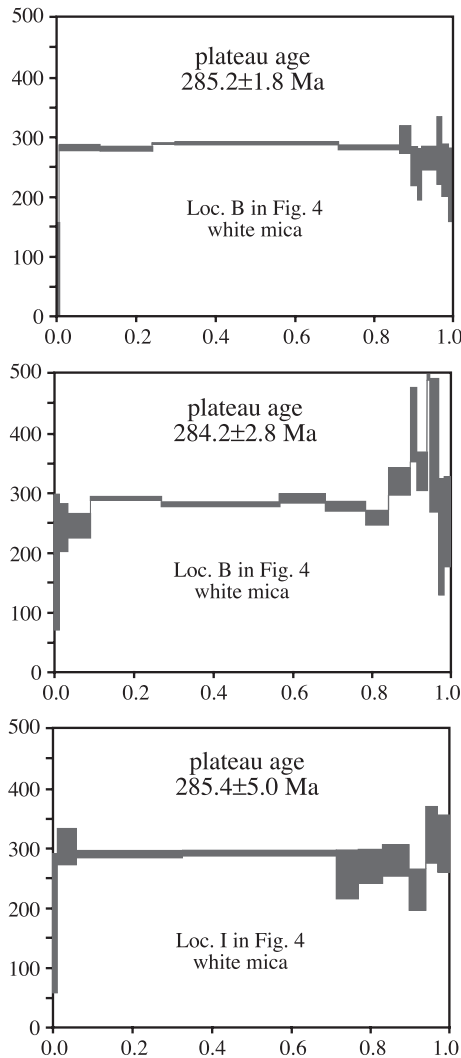


Fig. 6.  $^{40}\text{Ar}/^{39}\text{Ar}$  age spectra from metamorphic white mica. The two samples from location B are from outcrops about 3 km apart. Analytical methods and data are given in Appendices A and B.

stone and conglomerate (7%), and igneous rocks (<1%); metamorphic clasts are absent (Sunderlin, 2002). The chert clasts were most likely derived from Dillinger sources (Fig. 5E). Reed and Nelson (1980) reported Middle Devonian(?) megafossils from limestone clasts, which they linked to a limestone unit (Blodgett and Boucot, 1999) within what is now known as the Mystic subterranean. We processed three limestone clasts for conodonts, all of which yielded unexpectedly young, Pennsylvanian to earliest Permian

ages (Morrowan to Atokan, Morrowan to Desmoinesian, and Morrowan to earliest Permian) (Fig. 7 and Table 2). These were likely derived from limestones that locally comprise a minor part of the Upper Paleozoic of the Mystic subterranean (e.g., locality O in Fig. 2; Bundtzen et al., 1994).

Paleocurrents have been measured in two areas. At Mt. Dall (Fig. 2, locality J), clast imbrications (82 clasts) reveal that paleocurrents flowed toward the east, from a region underlain by outcrops of the Dillinger and Mystic subterraneans. In Medfra quadrangle (locality G in Figs. 2 and 3), clast imbrications (25

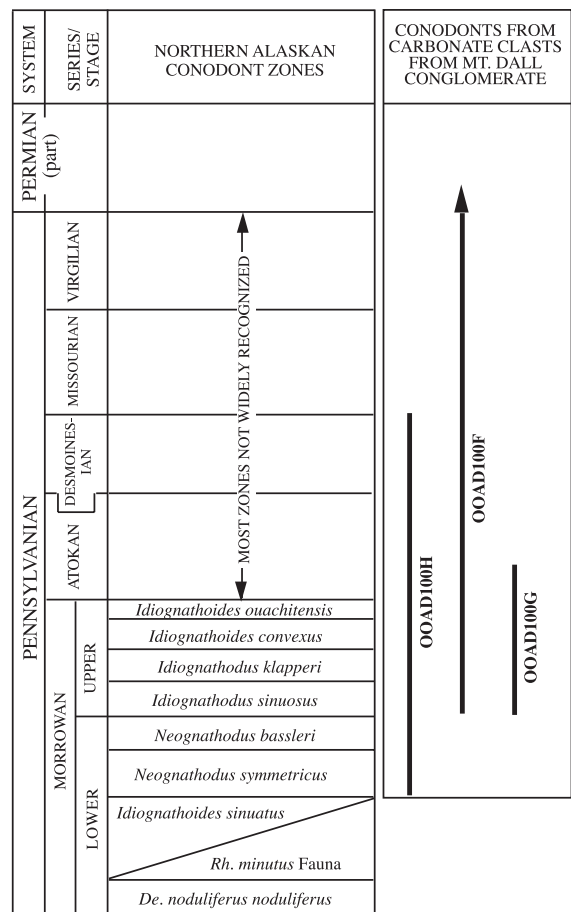


Fig. 7. Conodont age determinations on Pennsylvanian to possibly earliest Permian clasts in Mt. Dall conglomerate. All clasts are rounded limestone boulders, 20–30 cm in diameter. Limestones of this age range have been reported from the Mystic subterranean about 200 km to the southwest of Mt. Dall (locality O in Fig. 2). Fossil data are in Table 2.

Table 2

Lithologic description and conodont-based age and depositional environment of carbonate clasts from the Dahl Conglomerate

Lithology	Conodont fauna	Age	Conodont biofacies and depositional environment	Remarks
Rounded carbonate clast in conglomerate, 30 × 20 cm in size. Clast is medium-gray-weathering, medium-gray limestone with articulated crinoid columnals that have a maximum dimension of 7 mm in diameter by several cm long. Thin section is well-sorted, overpacked crinoid-bryozoan packstone.	1 juvenile, 2 subadult, and 1 adult fragment of <i>Idiognathodus</i> sp. indet. 10 indeterminate bar and blade fragments 25 ichthyoliths CAI: 4 <sup>a</sup> Field no.: 00AD100F; USGS colln. No. 33616-PC	late Morrowan (early Middle Pennsylvanian)-very Early Permian	Indeterminate (too few conodonts); the concentration of phosphatic skeletal elements suggests a lag concentrate.	Sample weight: 4.5 kg. Heavy-mineral concentrate: chiefly ichthyoliths, indeterminate phosphatic and phosphatized bioclasts, and lesser phosphatized rock fragments.
Rounded clast about 30 × 20 cm in size consisting of medium- to light-gray limestone with floating bioclasts. Thin section is bioturbated skeletal wackestone to packstone with local peloids; bioclasts are mainly diverse bryozoan and crinoid fragments, with minor ostracodes, gastropods, brachiopod spines, calcareous sponge spicules, and calcispheres.	3 juvenile Pa elements <i>Declinognathodus noduliferus</i> (Ellison and Graves) 1 subadult incomplete Pa element <i>Idiognathodus</i> sp. indet. <i>Idioproniodus conjunctus</i> (Gunnell) 1 P and 1 S element fragments 1 Pa element <i>Rhachistognathus minutus declinatus</i> Baesemann and Lane 5 juvenile Pa elements <i>Rhachistognathus minutus</i> (Higgins and Bouckaert) subsp. indet. 2 Pa element fragments <i>Rhachistognathus</i> sp. indet. 52 juvenile elements and indeterminate bar and blade fragments +60 ichthyoliths CAI: 4–4.5 Field no.: 00AD100G; USGS colln. No. 33617-PC	late Morrowan–early Atokan (early–middle Middle Pennsylvanian). This species association is similar to that of the upper half of the upper member of the Wahoo Limestone in the eastern Saddle River Mountains (see Krumhardt et al., 1996).	Indeterminate (too few conodonts); the conodonts present indicate a shoal- or near shoal-water depositional setting and the abundance of phosphatic material suggests a lag concentrate.	Sample weight: 4.5 kg. Heavy-mineral concentrate: chiefly ichthyoliths and indeterminate phosphatic bioclasts, with minor phosphatic brachiopod fragments and conodonts.
Rounded clast 20 × 20 cm in size consisting of medium- to medium-dark-gray limestone with scattered crinoid ossicles. Thin section is skeletal-oid grainstone; bioclasts are mainly crinoid and bryozoan fragments.	2 Pa element fragments <i>Neognathodus</i> ? sp. indet. 6 Pa element fragments <i>Adetognathus</i> sp. indet. 80 indeterminate bar, blade, and platform fragments 1 ichthyolith CAI: 4–4.5 Field no.: 00AD100H; USGS colln. No. 33618-PC	early, but not earliest, Morrowan–Desmoinesian (Early, but not earliest–late Middle Pennsylvanian)	Indeterminate (too few generically determinate conodonts); all conodonts are incomplete and some are considerably abraded, suggesting post-mortem transport within or from a relatively high-energy, shallow-water environment.	Sample weight: 3.3 kg. Heavy-mineral concentrate: phosphatized rock fragments and indeterminate bioclasts.

Clasts from lat. 62°35'40"N., long. 152°10'05"W., Talkeetna C-5 quadrangle, Alaska.

<sup>a</sup> CAI, conodont color alteration index; a CAI of 4 indicates the host rock reached at least 200 °C and a CAI of 4–4.5 indicates at least 230 °C (Epstein et al., 1997).

clasts) in a limestone-cobble conglomerate of probable Permian age (Andrews and Rishel, 1982) show paleoflow toward the southeast. Interestingly, limestone is no longer exposed to the northwest of this locality, only metamorphic rocks.

## 5. Discussion

### 5.1. The Browns Fork orogeny and Dall Basin

We here name the Pennsylvanian–Permian orogenic event in the northern Kuskokwim Mountains the “Browns Fork orogeny”, after the river in the Medfra quadrangle (Fig. 4). Likewise, we here name the Pennsylvanian–Permian siliciclastic basin in the Alaska Range the “Dall Basin”, after Mt. Dall. The original basin was probably much more extensive than the patchy present distribution of Pennsylvanian–Permian sandstone and conglomerate.

A simple, though non-unique model links the Browns Fork orogen and Dall Basin. A contractional orogen will inevitably depress the lithosphere to form a foreland basin. To our knowledge, the only Phanerozoic orogenic belts that entirely lack foreland basins are those that have so been deeply exhumed that no low-grade supracrustal rocks remain. According to this model, the Pennsylvanian–Permian metamorphic belt would be a vestige of the orogenic load, and the Pennsylvanian–Permian clastic rocks of the Mystic subterrane would represent the fill of the corresponding foreland basin. The great thicknesses, upward transition from flysch to molasse, and resedimented conglomerates all are typical of foreland basins. A lack of late Paleozoic volcanics in the Mystic subterrane would argue against a rift setting, the most obvious alternative. This lack of late Paleozoic magmatism in the Farewell terrane also would seem to rule out the possibility that tectonism was due to intra-arc shortening, and more likely due to collision.

Former continuity between the northern and southern areas of late Paleozoic tectonism cannot be demonstrated, but seems likely. The two places lie on opposite limbs of what Johnston (2001) called the Kulukbuk Hills orocline—a regional-scale bend in the map pattern of the Farewell terrane (Fig. 2). Although Johnston (2001) interpreted this to be a true orocline, i.e., a bend in an originally straighter orogen,

it has not been studied extensively. The map pattern is further complicated by regional NW–SE shortening, and by dextral displacements along the NE–SW striking Denali and Iditarod strike–slip faults (Miller et al., 2002). Although the late Paleozoic paleogeography is blurred by these younger events, we surmise that coeval areas of tectonism in the northern and southern parts of the Farewell terrane lined up end to end.

Thus, fragmentary evidence can be pieced together for a previously unrecognized Phanerozoic orogeny in Alaska, one that appears in none of the published scenarios for the assembly of the northern Cordillera (e.g., Plafker and Berg, 1994; Nokleberg et al., 2001). From Cambrian through Devonian, the Farewell terrane was a microcontinent with a passive margin that lay somewhere within an ocean between the Siberian and Laurentian cratons (Dumoulin et al., 2002)—a gap that later came to be clogged by a 4500-km-long, 1000-km-wide jumble of terranes (Johnston, 2001) (Fig. 1). By the Late Cretaceous, the Farewell had ended up in the midst of this jumble, part of a newly assembled bridge between two ancient cratons. The Browns Fork orogeny was an early event in this assembly.

### 5.2. Interactions between the Farewell terrane and its immediate neighbors

The weight of evidence suggests that the Browns Fork orogeny involved collision with something to the west (in modern coordinates). Paleocurrent data from late Paleozoic conglomerates (Fig. 2) show roughly west-to-east paleoflow in two widely separated areas, and the intensity of late Paleozoic metamorphism diminished eastward. Unfortunately, little is known about the late Paleozoic geology of the area immediately west of the Farewell terrane, because, except for a few fault slivers, the relevant rocks lie beneath many kilometers of turbidites of the Late Cretaceous Kuskokwim basin. About 75–100 km west of the Farewell terrane is a tract called the Innoko “terrane”. Patton et al. (1994) described this as a poorly exposed belt of ocean-floor and arc rocks ranging in age from Devonian to Early Cretaceous, which likely includes two unrelated assemblages. Although some rocks in the Innoko are too young to have participated in the Browns Fork orogeny, others are the right age and lithology to suggest, or at least permit, involvement. Miller and Bundtzen (1994) reported a hornblende

porphyry from Iditarod quadrangle (locality R in Fig. 2 and locality 11 in Fig. 1) that yielded an age of  $302 \pm 9$  Ma (K/Ar, hornblende). Permian graywacke has been described from the Ruby, Ophir, and Liven-good quadrangles (localities P and Q in Fig. 2 and localities 13 and 14 in Fig. 1) (Chapman and Patton, 1979; Bundtzen et al., 1997b; Weber et al., 1992). These volcanic and sedimentary rocks could represent an arc and an associated forearc basin or trench related to the Browns Fork orogeny.

The Yukon-Tanana “terrane” borders the Farewell terrane to the east (Fig. 2). It has long been treated as a single terrane (e.g., Coney et al., 1980), but in fact, it includes an early Paleozoic continental margin assemblage, a Devonian arc, an obducted late Paleozoic to Triassic ophiolite, metamorphic rocks of late Paleozoic to Triassic, Jurassic, and Early Cretaceous ages, and intrusives of Triassic, Jurassic, Cretaceous, and Tertiary ages (Dusel-Bacon et al., 2002). Evidence for late Paleozoic orogenesis is not known from the part of the Yukon-Tanana nearest the Farewell terrane. However, about 850 km to the east in Yukon Territory (locality 19 in Fig. 1), blueschist and eclogite have yielded  $^{40}\text{Ar}/^{39}\text{Ar}$  cooling ages of  $273 \pm 34$  and  $274 \pm 3$  Ma (Erdmer et al., 1998). Still farther east (locality 20 in Fig. 1), Murphy et al. (2002) recently documented Late Pennsylvanian west-directed thrusts that juxtapose different units within the Yukon-Tanana. Thus, distant parts of the Yukon-Tanana “terrane” were deformed and metamorphosed at the approximate time of the Browns Fork orogeny. However, the Jurassic and Early Cretaceous metamorphic events that affected the Yukon-Tanana in interior Alaska are unlike anything in the Farewell terrane. Late Paleozoic interactions between the Farewell and Yukon-Tanana cannot be demonstrated, and it is likely that the two were juxtaposed later.

The two other terranes that flank the Farewell terrane are also unlikely to have interacted with it during the Browns Fork orogeny. To the south, the Farewell is flanked by a Jurassic to mid-Cretaceous flysch belt (Kahiltna “terrane”) (Fig. 2), which marks the thickly sedimented suture zone between the Farewell terrane and Wrangellia (locality 16 in Fig. 1). Fossil ages in the flysch range from latest Jurassic to mid-Cretaceous (Turonian) and folds in the flysch are cross-cut by Late Cretaceous plutons. Collision between the Farewell terrane and Wrangellia is thus

inferred to have taken place during the Cretaceous, perhaps 200 million years after the Browns Fork orogeny. To the north, across an unmapped area of poor outcrop, the Farewell terrane is flanked by the Ruby terrane (Fig. 2), a Paleozoic continental margin assemblage that includes vestiges of a Devonian arc. The Ruby was metamorphosed to blueschist facies by 144 Ma and was intruded by granites at 118–109 Ma (Roeske et al., 1995). The Ruby shows no signs of a Permian orogeny, just as the Farewell terrane contains no record of Jura-Cretaceous blueschist conditions.

### 5.3. Late Paleozoic plate mosaic

Modern and ancient convergent plate boundaries connect to form belts that are thousands of kilometers long (e.g., circum-Pacific, Alpine-Himalaya, Innuitian-Caledonian-Appalachian). Thus, we would not expect the Browns Fork orogen to have existed in isolation. In addition to those already discussed, other areas of Late Pennsylvanian to Early Permian plate convergence that might have somehow linked up with the Browns Fork orogen are found in south-central Alaska, northeast Asia, and western Canada (Fig. 1).

The Uralian orogen and its extensions in Novaya Zemlya and Taimyr (localities 2, 4, and 6 in Fig. 1) together form one of the great collisional systems in Earth history, some 5500 km long. In that part of the Urals within the area of Fig. 1, and in Novaya Zemlya, the passive margin of Baltica collided with an outboard arc system, above an east-dipping subduction zone. The onset of collision is dated by the drowning of the passive margin beneath orogenically derived flysch, Late Pennsylvanian (Stephanian) in the northern Urals (locality 1 in Fig. 1), Early Permian (Artinskian) in Novaya Zemlya (locality 3 in Fig. 1) (Ziegler, 1989; Heafford, 1988). In Taimyr, the passive margin was on the Siberian side and the polarity of tectonic transport was opposite that in the rest of orogen. But the onset of orogeny was in the same age range, as shown (1) by Late Pennsylvanian to Early Permian thrusts and Permian granitic plutonism and metamorphism in the central Taimyr zone (locality 6 in Fig. 1) (Zonenshain et al., 1990) and (2) by foreland-basin sedimentation in the South Taimyr Trough that had commenced by Middle to Late Carboniferous (locality 5 in Fig. 1) (Posner, 1966). The eastern (Verkhoyansk) margin of the Siberian

craton (locality 7 in Fig. 1) apparently escaped collision until Late Jurassic (Sengor and Natalin, 1996, p. 556). Thus, if the convergent plate boundary in Taimyr continued any farther east, the record lies in the logjam (or “terrane wreck”—Johnston, 2001) of arcs and microcontinents now lodged between the ancient cratons of Siberia and Laurentia.

Evidence in this region for Late Pennsylvanian to Early Permian plate convergence includes arc magmatism, deformation, metamorphism, and sedimentation (Fig. 1). In northeast Asia, Permian arc volcanics are reported from the Okhotsk massif, and Carboniferous and Permian arc volcanics are reported from the Alazeya and Oloy terranes (localities 8, 9, and 10 in Fig. 1) (Sengor and Natalin, 1996, pp. 557–559). In south-central Alaska, Late Pennsylvanian and Early Permian volcanics define the Skolai Arc of Wrangellia (locality 16 in Fig. 1) (Nokleberg et al., 1994, pp. 355–356), which is interpreted to have formed above a subduction zone that dipped southwest (i.e., away from North America in present coordinates). Metamorphosed Permian arc volcanics in parts of the Stikine Terrane of British Columbia are dated at  $285 \pm 9$  Ma (locality 22 in Fig. 1) (Gareau et al., 1997). High-pressure metamorphic rocks of the Vedder Complex in northernmost Washington (locality 23 in Fig. 1) have yielded K–Ar ages of  $277 \pm 9$  and  $279 \pm 9$  on white mica and hornblende, respectively (Armstrong et al., 1983). Similarly, the high-pressure Garrison schist of northern Washington (locality 24 in Fig. 1) has yielded a hornblende K/Ar age of  $286 \pm 20$  Ma (Brandon et al., 1988). These fragments together support Ziegler’s (1989) conjecture that during the Late Pennsylvanian to Early Permian, the collision zone in Taimyr linked up with one or more convergent plate boundaries in the paleo-Pacific, offshore Laurentia.

## 6. Closing remarks

Reconnaissance field work in Alaska’s Farewell terrane has revealed evidence for a late Paleozoic orogenic belt (Browns Fork orogen) and a late Paleozoic foreland basin (Mt. Dall Basin). Neither of these was previously recognized, as they are in remote and poorly mapped country. We propose a link between the orogen and basin and suggest that orogeny

resulted from a collision between the Farewell terrane and rocks to the west (present coordinates). On a broader scale, we suggest that the Browns Fork orogen was part of a zone of plate convergence that stretched from the Urals to somewhere offshore the Cordilleran margin of North America.

## Acknowledgements

Most of the funding for this research was provided by the Mineral Resources Program of the U.S. Geological Survey. Sunderlin was supported, in addition, by grants from SEPM, the Paleontological Society, and the John T. Dillon Alaska Research Award of the Geological Society of America. Alison Till, Peter Haeussler, Stephen Johnston, and Terry Pavlis provided thoughtful reviews. Bill Patton generously shared maps, notes, thin sections, and samples. Joe Brinton did some of the  $^{40}\text{Ar}/^{39}\text{Ar}$  geochronology as part of a bachelor’s research project at University of Alaska, Fairbanks. Discussions with Fred Ziegler and Alison Till clarified our understanding of Taimyr stratigraphy and Alaskan metamorphism. Tom Rothfus assisted in the field. Warren Nokleberg provided us with digital maps of Alaskan and northeast Asian terranes. Phil Brease of Denali National Park helped us gain access to Mt. Dall. Jack and Sherri Hayden of Denali West Lodge provided logistical support.

## Appendix A

For  $^{40}\text{Ar}/^{39}\text{Ar}$  analysis, samples were crushed, washed, sieved, and hand-picked to ensure selection of pure, clean minerals. The samples were wrapped in aluminum foil and within aluminum cans of 2.5 cm diameter and 6 cm height. Standard monitor minerals were used to monitor the neutron flux. The samples were irradiated in position 5c of the uranium-enriched research reactor of McMaster University in Hamilton, Ontario, Canada.

Upon their return from the reactor, the sample and monitors were loaded into 2-mm diameter holes in a copper tray, which was then loaded in an ultra-high vacuum extraction line. The monitor mineral MMhb-1 with an age of 513.9 Ma was used. The monitors were

fused, and samples heated, using a 6 W argon-ion laser following the technique described in York et al. (1981) and Lauer et al. (1987). Argon purification was achieved using a liquid nitrogen cold trap and a SAES Zr–Al getter at 400°C. The samples were then analyzed in a VG-3600 mass spectrometer at the Geophysical Institute, University of Alaska Fairbanks (Lauer, 2000). The argon isotopes measured were corrected for system blank and mass discrimination, as well as calcium, potassium, and chlorine interference reactions following procedures outlined in McDougall and Harrison (1999).

A summary of all the  $^{40}\text{Ar}/^{39}\text{Ar}$  results is given in Table 1, with all ages quoted to the  $\pm 1$  sigma level and calculated using the constants of Steiger and Jaeger (1977). Analytical results are tabulated in Appendix B. Integrated age is the weighted average of all gas fractions. This often includes fractions where argon loss occurs and therefore may not represent an original age or a reset age. Plateau age is determined from 3 or more consecutive fractions whose ages are within 2 sigma of each other (MSWD generally less than  $\sim 2$ ) and total more than 50% of gas release.

Appendix B.  $^{40}\text{Ar}/^{39}\text{Ar}$  data

3-7-1C White Mica								Weighted average of J from standards=0.009356 ± 0.000039								
Laser Power (mW)	Cumulative <sup>39</sup> Ar	<sup>40</sup> Ar/ <sup>39</sup> Ar measured	+/-	<sup>37</sup> Ar/ <sup>39</sup> Ar measured	+/-	<sup>36</sup> Ar/ <sup>39</sup> Ar measured	+/-	% Atm. <sup>40</sup> Ar	Ca/K	+/-	Cl/K	+/-	<sup>40</sup> Ar*/ <sup>39</sup> Ar <sub>K</sub>	+/-	Age (Ma)	+/- (Ma)
150	0.001	18.546	3.776	-0.775	0.605	0.1024	0.0902	163.7	-1.421	1.109	0.016	0.022	-11.781	26.153	-210.7	496.1
300	0.009	18.276	0.644	0.018	0.129	0.0456	0.0165	73.9	0.033	0.237	-0.002	0.002	4.763	4.872	78.7	78.7
500	0.111	18.700	0.106	-0.009	0.011	0.0019	0.0012	2.9	-0.016	0.020	0.000	0.000	18.125	0.355	282.6	5.1
750	0.243	18.464	0.132	0.002	0.006	0.0018	0.0007	2.9	0.004	0.012	0.000	0.000	17.901	0.242	279.4	3.5
1000	0.708	18.654	0.060	0.000	0.002	0.0004	0.0003	0.6	0.000	0.004	0.001	0.000	18.521	0.095	288.3	1.4
1250	0.864	18.098	0.049	-0.001	0.007	0.0002	0.0009	0.4	-0.002	0.012	0.000	0.000	18.001	0.266	280.8	3.8
1500	0.892	17.320	0.369	-0.052	0.029	-0.0057	0.0053	-9.7	-0.095	0.053	-0.001	0.001	18.977	1.603	294.9	23.0
1750	0.909	18.265	0.550	0.016	0.056	0.0080	0.0075	13.0	0.029	0.102	-0.001	0.002	15.862	2.273	249.6	33.4
2000	0.921	17.161	0.355	-0.027	0.072	0.0074	0.0096	12.8	-0.050	0.133	-0.003	0.003	14.941	2.847	236.1	42.2
2500	0.961	18.246	0.326	-0.004	0.022	0.0045	0.0043	7.3	-0.007	0.040	0.000	0.001	16.882	1.317	264.6	19.2
3000	0.971	17.489	0.387	-0.052	0.080	-0.0008	0.0131	-1.4	-0.095	0.147	-0.003	0.003	17.696	3.893	276.4	56.4
5000	0.989	18.311	0.489	0.022	0.036	0.0097	0.0099	15.7	0.040	0.066	-0.002	0.003	15.420	2.960	243.1	43.7
8000	1.000	18.976	1.123	-0.006	0.071	0.0175	0.0136	27.3	-0.011	0.130	0.001	0.004	13.782	4.084	218.8	61.1
Integrated		18.451	0.044	-0.003	0.003	0.0017	0.0005	2.8	-0.006	0.006	0.000	0.000	17.915	0.150	279.6	2.4

3-3-1C White Mica								Weighted average of J from standards=0.009356 ± 0.000039								
Laser Power (mW)	Cumulative <sup>39</sup> Ar	<sup>40</sup> Ar/ <sup>39</sup> Ar measured	+/-	<sup>37</sup> Ar/ <sup>39</sup> Ar measured	+/-	<sup>36</sup> Ar/ <sup>39</sup> Ar measured	+/-	% Atm. <sup>40</sup> Ar	Ca/K	+/-	Cl/K	+/-	<sup>40</sup> Ar*/ <sup>39</sup> Ar <sub>K</sub>	+/-	Age (Ma)	+/- (Ma)
100	0.003	13.268	2.573	0.005	0.588	0.0367	0.1085	81.9	0.010	1.079	0.004	0.024	2.396	32.018	40.0	528.6
150	0.007	15.562	1.882	0.047	0.218	0.0324	0.0506	61.6	0.086	0.399	0.005	0.013	5.972	14.958	98.1	239.1
200	0.016	17.756	0.786	-0.021	0.143	0.0211	0.0251	35.1	-0.039	0.263	0.008	0.006	11.497	7.437	184.3	113.4
300	0.038	19.177	0.496	-0.028	0.050	0.0130	0.0093	20.0	-0.052	0.093	0.003	0.002	15.312	2.781	241.6	41.1
450	0.096	18.782	0.219	0.012	0.017	0.0109	0.0048	17.1	0.022	0.031	0.001	0.001	15.539	1.421	244.9	20.9
600	0.273	18.409	0.081	-0.002	0.006	-0.0009	0.0010	-1.5	-0.003	0.010	0.000	0.000	18.657	0.308	290.3	4.4
750	0.568	18.271	0.107	-0.002	0.003	0.0009	0.0008	1.5	-0.004	0.005	0.000	0.000	17.975	0.244	280.4	3.5
900	0.682	18.285	0.193	-0.006	0.006	-0.0015	0.0019	-2.4	-0.012	0.012	-0.001	0.001	18.699	0.580	290.9	8.3
1050	0.785	18.150	0.207	0.002	0.010	0.0012	0.0017	2.0	0.004	0.018	0.000	0.001	17.756	0.547	277.3	7.9
1200	0.843	18.061	0.224	0.023	0.016	0.0053	0.0029	8.7	0.043	0.029	0.001	0.001	16.471	0.880	258.6	12.9
1350	0.899	18.730	0.380	-0.005	0.019	-0.0070	0.0052	-11.0	-0.010	0.035	0.001	0.001	20.759	1.578	320.2	22.3
1500	0.914	19.296	0.789	0.009	0.082	-0.0282	0.0154	-43.2	0.017	0.151	0.001	0.004	27.594	4.672	414.3	62.7
1650	0.941	19.506	0.536	0.023	0.046	-0.0083	0.0076	-12.6	0.042	0.085	0.003	0.002	21.926	2.334	336.6	32.7
1800	0.947	18.930	1.400	0.059	0.235	-0.0939	0.0462	-146.8	0.108	0.432	0.002	0.013	46.658	13.925	653.5	163.6

(continued on next page)

## Appendix B (continued)

3-3-1C White Mica								Weighted average of J from standards = 0.009356 ± 0.000039								
Laser Power (mW)	Cumulative <sup>39</sup> Ar	<sup>40</sup> Ar/ <sup>39</sup> Ar measured	+ / −	<sup>37</sup> Ar/ <sup>39</sup> Ar measured	+ / −	<sup>36</sup> Ar/ <sup>39</sup> Ar measured	+ / −	% Atm. <sup>40</sup> Ar	Ca/K	+ / −	Cl/K	+ / −	<sup>40</sup> Ar*/ <sup>39</sup> Ar <sub>K</sub>	+ / −	Age (Ma)	+ / − (Ma)
2000	0.970	18.965	0.424	− 0.018	0.047	− 0.0209	0.0276	− 32.5	− 0.033	0.086	0.002	0.003	25.097	8.181	380.5	111.8
3500	0.985	21.149	0.668	− 0.023	0.092	0.0230	0.0219	32.2	− 0.043	0.168	0.004	0.005	14.323	6.482	226.9	96.5
8500	1.000	19.796	0.618	0.037	0.086	0.0127	0.0174	19.0	0.067	0.158	0.003	0.006	16.016	5.151	251.9	75.6
Integrated		18.455	0.062	0.000	0.005	0.0002	0.0012	0.3	0.001	0.009	0.001	0.000	18.367	0.344	286.1	5.1
2-3-1C White Mica								Weighted average of J from standards = 0.009356 ± 0.000039								
Laser Power (mW)	Cumulative <sup>39</sup> Ar	<sup>40</sup> Ar/ <sup>39</sup> Ar measured	+ / −	<sup>37</sup> Ar/ <sup>39</sup> Ar measured	+ / −	<sup>36</sup> Ar/ <sup>39</sup> Ar measured	+ / −	% Atm. <sup>40</sup> Ar	Ca/K	+ / −	Cl/K	+ / −	<sup>40</sup> Ar*/ <sup>39</sup> Ar <sub>K</sub>	+ / −	Age (Ma)	+ / − (Ma)
150	0.002	14.941	4.045	0.548	0.746	0.0861	0.2518	170.2	1.005	1.370	0.058	0.054	− 10.478	74.318	− 186.2	1390.8
300	0.015	17.445	0.720	0.471	0.133	0.0228	0.0255	38.4	0.865	0.244	0.009	0.005	10.724	7.556	172.5	115.9
500	0.062	18.414	0.377	0.097	0.035	− 0.0035	0.0072	− 5.7	0.178	0.063	− 0.002	0.002	19.431	2.154	301.4	30.8
750	0.330	18.885	0.126	0.018	0.005	0.0011	0.0012	1.7	0.033	0.010	0.000	0.000	18.536	0.374	288.5	5.4
1000	0.714	18.942	0.147	0.011	0.005	0.0010	0.0009	1.5	0.021	0.009	0.000	0.000	18.628	0.314	289.9	4.5
1250	0.770	18.623	0.604	0.012	0.023	0.0082	0.0091	13.0	0.023	0.042	− 0.002	0.001	16.176	2.743	254.3	40.2
1500	0.832	19.108	0.390	0.035	0.036	0.0067	0.0064	10.3	0.063	0.065	− 0.003	0.001	17.114	1.934	268.0	28.1
1750	0.899	19.037	0.332	0.009	0.029	0.0042	0.0061	6.5	0.017	0.053	0.001	0.002	17.765	1.824	277.4	26.4
2000	0.942	18.949	0.711	0.017	0.043	0.0150	0.0074	23.5	0.030	0.078	0.001	0.001	14.482	2.286	229.3	34.0
2500	0.973	19.388	0.609	0.004	0.105	− 0.0048	0.0112	− 7.4	0.006	0.193	− 0.002	0.002	20.784	3.364	320.6	47.5
3000	1.000	19.975	0.551	0.064	0.124	0.0008	0.0111	1.1	0.118	0.228	0.002	0.003	19.726	3.330	305.6	47.5
Integrated		18.917	0.092	0.027	0.007	0.0026	0.0012	4.1	0.049	0.013	0.000	0.000	18.121	0.374	282.6	5.5

## NOTES:

Weighted average J (irradiation parameter) calculated from standard mmhb-1 (513.9 Ma).

Laser power (in milliwatts) is the heating step from a defocussed argon-ion laser. The last step represents fusion of the sample.

Measured isotopic ratios (and 1-sigma error) are corrected for reactor induced interferences and decay of <sup>37</sup>Ar and <sup>39</sup>Ar.

% Atm. <sup>40</sup>Ar: percent of atmospheric <sup>40</sup>Ar in the sample assuming an initial <sup>40</sup>Ar/<sup>36</sup>Ar ratio of 295.5.

<sup>40</sup>Ar\*/<sup>39</sup>Ar<sub>K</sub> and ages (and 1-sigma errors) calculated using the equations and constants quoted in McDougall and Harrison (1999).

Correction factors:

$$(^{39}\text{Ar}/^{37}\text{Ar})_{\text{Ca}} = 0.000651 \pm 3.1\text{e-}05$$

$$(^{36}\text{Ar}/^{37}\text{Ar})_{\text{Ca}} = 0.000254 \pm 9\text{e-}06$$

$$(^{40}\text{Ar}/^{39}\text{Ar})_{\text{K}} = 0.0287 \pm 0.0055$$

Fractions used in calculation of plateau shown in bold.

## References

- Andrews, T., Rishel, J., 1982. Reef Ridge 1–13 project areas, Kuskokwim Block. Anchorage, Alaska, Patino, Annual Report (1981), vol. 1. 49 pp.
- Armstrong, R.L., Harakal, J.E., Brown, E.H., Bernardi, M.L., Rady, P.M., 1983. Late Paleozoic high-pressure metamorphic rocks in northwestern Washington and southwestern British Columbia: the Vedder Complex. *Geological Society of America Bulletin* 94, 451–458.
- Blodgett, R.B., Boucot Jr., A.J., 1999. Late Early Devonian (late Emsian) eospiriferinid brachiopods from Shellabarger Pass, Talkleetna C-6 quadrangle, Denali National Park, Alaska and their paleogeographic importance: further evidence for a Siberian origin of the Farewell and allied Alaskan accreted terranes. *Senckenbergiana Lethaea* 79, 209–221.
- Blodgett, R.B., Rohr, D.M., Boucot, A.J., 2002. Paleozoic links among some Alaskan accreted terranes and Siberia based on megafossils. In: Miller, E., et al. (Eds.), *Tectonic Evolution of the Bering Shelf-Chukchi Sea-Arctic Margin and Adjacent Landmasses*. Geological Society of America, Boulder, CO, Special Paper, vol. 360, pp. 273–280.
- Box, S.E., 1985. Early Cretaceous orogenic belt in northwestern Alaska: Internal organization, lateral extent and tectonic interpretation. In: Howell, D.G. (Ed.), *Tectonostratigraphic Terranes of the Circum-Pacific Region*. Circum-Pacific Council for Energy and Mineral Resources. Earth Science Series, Houston, TX, vol. 1, pp. 137–145.
- Brandon, M.T., Cowan, D.S., Vance, J.A., 1988. The Late Cretaceous San Juan thrust system, San Juan Islands, Washington. Geological Society of America, Boulder, CO, Special Paper, vol. 221. 81 pp.
- Bundtzen, T.K., Gilbert, W.G., 1983. Outline of geology and mineral resources of upper Kuskokwim region, Alaska. *Journal of the Alaska Geological Society* 3, 101–117.
- Bundtzen, T.K., Laird, G.M., Blodgett, R.B., Clautice, K.H., Harris, E.E., 1994. Geologic map of the Gagaryah River area, Lime Hills C-5 and C-6 quadrangles, southwestern Alaska. Alaska Division of Geological and Geophysical Surveys Public-Data File 94-40, 16 pp., scale 1:63,360.
- Bundtzen, T.K., Harris, E.E., Gilbert, W.G., 1997a. Geologic map of the eastern half of the McGrath quadrangle, Alaska. Alaska Division of Geological and Geophysical Surveys Report of Investigations 97-14a, 38 pp., scale 1:125,000.
- Bundtzen, T.K., Pinney, D.A., Laird, G.M., 1997b. Preliminary geologic map and data tables from the Ophir C-1 and western Medfra C-6 quadrangles, Alaska. Alaska Division of Geological and Geophysical Surveys Public-Data File 97-46.
- Chapman, R.M., Patton Jr., W.W., 1979. Two upper Paleozoic sedimentary rock units identified in the southwestern part of the Ruby quadrangle. U.S. Geological Survey Circular 80-B, B59–B61.
- Coney, P.J., Jones, D.L., Monger, J.W.H., 1980. Cordilleran suspect terranes. *Nature* 288, 29–33.
- Decker, J., Bergman, S.C., Blodgett, R.B., Box, S.E., Bundtzen, T.K., Clough, J.G., Coonrad, W.L., Gilbert, W.G., Miller, M.L., Murphy, J.M., Robinson, M.S., Wallace, W.K., 1994. Geology of southwestern Alaska. In: Plafker, G., Berg, H.C. (Eds.), *The Geology of Alaska*. Geological Society of America, Boulder, CO, DNAG Series, vol. G-1, pp. 285–310.
- Dillon, J.T., Patton Jr., W.W., Muksa, S.B., Tilton, G.R., Blum, J., Moll, E.T., 1985. New radiometric evidence for the age and thermal history of the metamorphic rocks of the Ruby and Nixon Fork terranes, west-central Alaska. U.S. Geological Survey Circular 945, 13–18.
- Dumoulin, J.A., Harris, A.G., Gagiev, M., Bradley, D.C., Repetski, J.E., 2002. Lithostratigraphic, conodont, and other faunal links between lower Paleozoic strata in northern and central Alaska and northeastern Russia. In: Miller, E., et al. (Eds.), *Tectonic Evolution of the Bering Shelf-Chukchi Sea-Arctic Margin and Adjacent Landmasses*. Geological Society of America, Boulder, CO, Special Paper, vol. 360, pp. 291–312.
- Dusel-Bacon, C., Lanphere, M.A., Sharp, W.D., Layer, P.W., Hansen, V.L., 2002. Mesozoic thermal history and timing of structural events for the Yukon-Tanana Upland, east-central Alaska:  $^{40}\text{Ar}/^{39}\text{Ar}$  data for metamorphic and plutonic rocks. *Canadian Journal of Earth Science* 39, 1013–1051.
- Epstein, A.G., Epstein, J.B., Harris, L.D., 1977. Conodont color alteration—an index to organic metamorphism. U.S. Geological Survey Professional Paper 995. 27 pp.
- Erdmer, P., Ghent, E.D., Archibald, D.A., Stout, M.Z., 1998. Paleozoic and Mesozoic high-pressure metamorphism at the margin of ancestral North America in central Yukon. *Geological Society of America Bulletin* 110, 615–629.
- Gareau, S.A., Friedman, R.M., Woodsworth, G.J., Childe, F., 1997. U–Pb ages from the northeastern quadrant of terrace map-area, west-central British Columbia. *Geological Survey of Canada* 97-1A, 31–40.
- Heafford, A.P., 1988. Carboniferous through Triassic stratigraphy of the Barents Shelf. In: Harland, W.B., Dowdeswell, E.K. (Eds.), *Geological Evolution of the Barents Shelf Region*. Graham and Trotman, London, pp. 89–108.
- Johnson, G.L., Churkin, M.J., 1976. Sheet 19, Arctic, in Chubert, G., and Faure-Muret, A., co-ordinators, *Atlas Géologique du Monde*. UNESCO, scale 1:10,000,000.
- Johnston, S.T., 2001. The great Alaskan terrane wreck: reconciliation of paleomagnetic and geologic data in the northern Cordillera. *Earth and Planetary Science Letters* 193, 259–272.
- Jones, D.L., Silberling, N.J., Coney, P.J., Plafker, G.W., 1987. Lithotectonic terrane map of Alaska, west of the 141st meridian. U.S. Geological Survey Map MF-1874-A, scale 1:2,500,000.
- Krumhardt, A.P., Harris, A.G., Watts, K.F., 1996. Lithostratigraphy, microlithofacies, and conodont biostratigraphy and biofacies of the Wahoo Limestone (Carboniferous), eastern Sadlerochit Mountains, northeast Brooks Range, Alaska: U.S. Geological Survey Professional Paper 1568. 71 pp.
- Layer, P.W., 2000. Argon-40/argon-39 age of the El'gygytyn impact event, Chukotka, Russia. *Meteoritics & Planetary Science* 35, 591–599.
- Layer, P.W., Hall, C.M., York, D., 1987. The derivation of  $^{40}\text{Ar}/^{39}\text{Ar}$  age spectra of single grains of hornblende and biotite by laser step heating. *Geophysical Research Letters* 14, 757–760.
- Mamay, S.H., Reed, B.L., 1984. Permian plant megafossils from

- the conglomerate of Mt. Dall, central Alaska Range. U.S. Geological Survey Circular 868, 98–102.
- McClelland, W.C., Kusky, T., Bradley, D.C., Dumoulin, J., Harris, A.G., 1999. The nature of Nixon Fork “basement”, west-central Alaska. *Geological Society of America, Abstracts with Programs* 31 (6), A-78.
- McDougall, I., Harrison, T.M., 1999. *Geochronology and Thermochronology by the  $^{40}\text{Ar}/^{39}\text{Ar}$  Method*, 2nd ed. Oxford Univ. Press, New York. 269 pp.
- Miller, M.L., Bundtzen, T.K., 1994. Generalized geologic map of the Iditarod quadrangle, Alaska, showing potassium-argon, major oxide, trace element, fossil, paleocurrent, and archaeological sample localities. U.S. Geological Survey Map MF-2219-A, 48 p., scale 1:250,000.
- Miller, M.L., Bradley, D.C., Bundtzen, T.K., McClelland, W., 2002. Late Cretaceous through Cenozoic strike-slip tectonics of southwestern Alaska. *Journal of Geology* 110, 247–270.
- Murphy, D.C., Colpron, M., Roots, C., Gordey, S.P., Abbott, J.G., 2002. Finlayson lake targeted geoscience initiative (southeastern Yukon), Part 1: Bedrock geology. In: Edmond, D.S., et al. (Eds.), *Yukon Exploration and Geology 2001*. Exploration and Geological Services Division, Indian and Northern Affairs Canada, Whitehorse, Yukon, pp. 189–207.
- Nokleberg, W.J., Plafker, G., Wilson, F.H., 1994. Geology of south-central Alaska. In: Plafker, G., Berg, H.C. (Eds.), *The Geology of Alaska*. Geological Society of America, Boulder, CO, DNAG Series, vol. G-1, pp. 311–366.
- Nokleberg, W.J., Parfenov, L.M., Monger, J.W.H., Norton, I.O., Khanchuk, A.I., Stone, D.B., Scotese, C.R., Scholl, D.W., Fujita, K., 2001. Phanerozoic tectonic evolution of the circum-North Pacific. U.S. Geological Survey Professional Paper, vol. 1626. 122 pp.
- Patton Jr., W.W., Dutro Jr., J.T., 1979. Age of the metamorphic complex in the northern Kuskokwim Mountains, west-central Alaska. U.S. Geological Survey Circular 804-B, B61–B63.
- Patton, W.W., Jr., Moll, E.J., Dutro, J.T., Jr., Silberman, M.L., Chapman, R.M., 1980. Preliminary geologic map of the Medfra quadrangle, Alaska. U.S. Geological Survey Open-File Report 80-811A, scale 1:250,000.
- Patton, W.W., Box, S.E., Moll-Stalcup, E.J., Miller, T.P., 1994. Geology of west-central Alaska. In: Plafker, G., Berg, H.C. (Eds.), *The Geology of Alaska*. Geological Society of America, Boulder, CO, DNAG Series, vol. G-1, pp. 241–269.
- Plafker, G., Berg, H.C., 1994. Overview of the geology and tectonic evolution of Alaska. In: Plafker, G., Berg, H.C. (Eds.), *The Geology of Alaska*. Geological Society of America, Boulder, CO, DNAG Series, vol. G-1, pp. 989–1021.
- Posner, V.M. (Ed.), 1966. Paleotectonic map of the USSR, Middle and Late Carboniferous, in Vinogradov, A.P. (editor in chief), 1968. *The Atlas of Lithological-Paleogeographical Maps of the USSR*, Ministry of Geology of the USSR, v. 2.
- Reed, B.L., Nelson, S.W., 1980. Geologic map of the Talkeetna quadrangle, Alaska. U.S. Geological Survey Map I-1174, 15 p., scale 1:250,000.
- Roeske, S.M., Dusel-Bacon, C., Aleinikoff, J.N., Snee, L.W., Lanphere, M.A., 1995. Metamorphic and structural history of continental crust at a Mesozoic collisional margin, the Ruby terrane, central Alaska. *Journal of Metamorphic Geology* 13, 5–40.
- Sengor, A.M.C., Natalin, B.A., 1996. Paleotectonics of Asia: Fragments of a synthesis. In: Yin, A. and Harrison, T.M.M. (Eds.), *The Tectonic Evolution of Asia*. Cambridge, Cambridge Univ. Press, Rubey Colloquium, pp. 486–640.
- Silberling, N.J., Jones, D.L., Monger, J.W.H., Coney, P.J., Berg, H.C., Plafker, G., 1994. Lithotectonic terrane map of Alaska and adjacent parts of Canada. In: Plafker, G., Berg, H.C. (Eds.), *The Geology of Alaska*. Geological Society of America, Boulder, CO, DNAG Series, vol. G-1, plate 3, scale 1:2,500,000.
- Silberman, M.L., Moll, E.J., Patton, W.W., Chapman, R.M., Connor, C.L., 1979. Precambrian age of metamorphic rocks from the Ruby province, Medfra and Ruby quadrangles; preliminary evidence from radiometric age data. U.S. Geological Survey Circular 804-B, B66–B67.
- Soja, C.M., Antoshkina, A.I., 1997. Coeval development of Silurian stromatolite reefs in Alaska and the Ural Mountains: implications for paleogeography of the Alexander terrane. *Geology* 25, 539–542.
- Steiger, R.H., Jaeger, E., 1977. Subcommittee on geochronology: convention on the use of decay constants in geo and cosmochronology. *Earth and Planet Science Letters* 36, 359–362.
- Sunderlin, D., 2002. A sedimentary characterization of the Mt. Dall Conglomerate, Farewell terrane, Alaska, and its paleoenvironmental implications. *Geological Society of America, Abstracts with Programs* 34 (6), 282.
- Torsvik, T.H., Tait, J., Moralev, V.M., McKerrow, W.S., Sturt, B.A., 1995. Ordovician paleogeography of Siberia and adjacent continents. *Journal of the Geological Society of London* 152, 279–287.
- Weber, F.R., Wheeler, K.L., Rinehart, C.D., Chapman, R.M., Blodgett, R.B., 1992. Geologic map of the Livengood quadrangle, Alaska. U.S. Geological Survey Open-File Report 92-562, 20 pp., scale 1:250,000.
- Wilson, F.H., Dover, J.H., Bradley, D.C., Weber, F.R., Bundtzen, T.K., Haeussler, P.J., 1998. Geologic map of central (interior) Alaska: U.S. Geological Survey Open-File Report 98–133, 64 p., 3 plates, scale 1:500,000 (also released as a CD-ROM).
- York, D., Hall, C.M., Yanase, Y., Hanes, J.A., Kenyon, W.J., 1981.  $^{40}\text{Ar}/^{39}\text{Ar}$  dating of terrestrial minerals with a continuous laser. *Geophysical Research Letters* 8, 1136–1138.
- Ziegler, P.A., 1989. *Evolution of Laurussia*. Kluwer Academic Publishing, Dordrecht, the Netherlands. 102 pp.
- Zonenshain, L.P., Kuzmin, M.I., Natapov, L.M., 1990. *Geology of the USSR: a plate tectonic synthesis*. American Geophysical Union, Geodynamics Series 21. 242 pp.